Journal of Molecular Structure 1009 (2012) 42–48

Contents lists available at SciVerse ScienceDirect

Journal of Molecular Structure

journal homepage: www.elsevier.com/locate/molstruc

IR spectra and structure of 2-{5,5-dimethyl-3-[(2-phenyl)vinyl]cyclohex-2-enylidene}-malononitrile and its potassium cyanide and sodium methoxide carbanionic adducts: Experimental and B3LYP theoretical studies

Simeon S. Stoyanov *, Jordan A. Tsenov, Denitsa Y. Yancheva

Department of Structural Organic Analysis, Institute of Organic Chemistry with Centre of Phytochemistry, Bulgarian Academy of Sciences, Acad. G. Bonchev Str., Build. 9, 1113 Sofia, Bulgaria

ARTICLE INFO

Article history:
Available online 17 September 2011

Keywords:
IR
DFT B3LYP
2-{5,5-Dimethyl-3-[(2-phenyl)vinyl]-cyclohex-2-enylidene}-malononitrile
Carbanionic adducts
Isomerization

ABSTRACT

A combined IR experimental/B3LYP computational approach was applied to follow the formation and isomerization of potassium cyanide and sodium methoxide carbanionic adducts of 2-{5,5-dimethyl-3-[(2-phenyl)vinyl]cyclohex-2-enylidene}-malononitrile **1**. A very good agreement was found between theoretical and experimental IR data about neutral compound **1**. In agreement between theory and experiment, **1** forms β-, δ-, and ζ-adducts with the above mentioned nucleophiles. Structural changes and energy differences between various adducts and their diastereoisomers, have also been studied. According to the computations, the chemical driving force in the β → δ and δ → ζ isomerisation is the higher stability of the corresponding adducts by *c.a.* 10 kJ mol^{-1} and *c.a.* 30 kJ mol^{-1}, respectively.

1. Introduction

2-{5,5-Dimethyl-3-[(2-phenyl)vinyl]cyclohex-2-enylidene}-malononitrile **1**, see Scheme 1, was prepared first by Lemke in 1970 as a precursor in the Knoevenagel-type synthesis of a large series of its 12-ylidene derivates [1–3]. These derivates are high-quality dyes for synthetic polymers [1–3]; some of these dyes have solvatochromic properties [1–3]. Nowadays 12-ylidene derivates of **1** are of special interest as non-linear optical [4–17] and fluorescent [10] materials. Experimental and theoretical (B3LYP/6-31G*), IR (solid state) and Raman spectra of **1** have been studied previously in detail [8]; some 12-ylidene derivates of **1** have also been studied thoroughly by IR [8–10], polarized IR [9] and Raman [8] spectroscopy, B3LYP quantum-chemical calculations [7,8,10] and single-crystal X-ray diffraction [11–17].

On the other hand, it is well known [18] that nucleophilic attacks to C=C bonds are favoured by electron-accepting substituents, where A, Nu$^-$ and E$^+$ are the acceptor, nucleophile and electrophile, respectively.

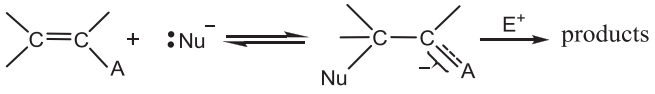

2

When the nucleophilic attacks take place in aprotic solvents (E$^+$ is usually H$^+$) the intermediate adducts **2** have been isolated in many cases [18–25]. Both, sodium methoxide (Nu$^-$≡CH_3O^-) [24,25] and potassium cyanide (Nu$^-$≡CN^-) [26–29] carbanionic adducts of benzylidenemalononitrile [24] and other strongly polarized alkenes [22–30], butadienes and hexatrienes [24] have been studied. Nucleophilic attacks by uncharged Lewis bases Nu: result in the formation of zwitterions **3**.

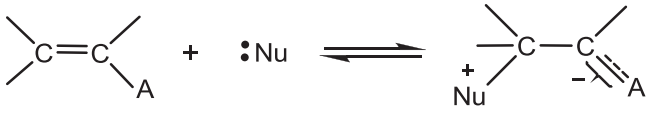

3

This result has been established in cases of tertialy phosphine adducts (**3**, Nu$^-$≡R_3P:) of benzylidenemalononitrile **4** (Scheme 2) by IR [31–33], NMR [34] and confirmed by X-ray diffraction [35]. The heptylamine zwitterionic adduct (Nu$^-$≡$C_7H_{15}NH_2^-$) of the same compound has also been studied by IR spectra [26]. Juchnovski and Binev [24] found that 1,1-dicyano-4-phenylbutadiene **5** (Scheme 2) and other strongly polarized conjugated butadienes react with CH_3ONa to form the β-adduct. Within 24 h, however, it isomerises spontaneously and practically completely into the corresponding δ-adduct. The authors [24] supposed that the isomerisation was provoked by the higher stability of δ-adduct, due to larger delocalization of the carbanionic charge in δ-adduct,

* Corresponding author.
E-mail address: s_stoyanov@orgchm.bas.bg (S.S. Stoyanov).

0022-2860/$ - see front matter © 2011 Published by Elsevier B.V.
doi:10.1016/j.molstruc.2011.08.048

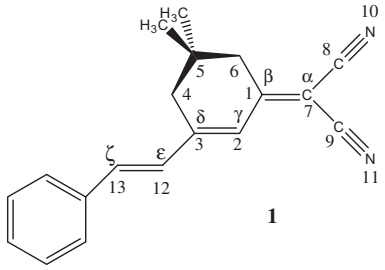

Scheme 1. Chemical structure and atom numbering of **1.**

compared to β-adduct. This supposition was confirmed later by ab initio HF energy analysis [36].

The β-adduct, oxyanion, and adduct-anion of 4-hidroxy benzylidenemalononitrile **6** (Scheme 2) have also been studied [28]. The authors [28] found that the HF method gave a good agreement between computed and observed IR frequencies for **6**. The mean absolute deviations for **6** and its adduct were 15 and 10 cm^{-1} respectively. In our previous study [37] we prepared β- and δ-adducts of 3,5,5-trimethyl(cyclohex-2-enylidene) malononitrile **7** (Scheme 2). We found, that the B3LYP functional predicts much better the IR frequencies of **7** and its adducts than the HF method predicted them for compounds **4–6** [25,27,36]. Recently, we found new B3LYP scale factors and equations for cyano IR frequencies and intensities [38].

The title compound **1** is formally an analogue of **7**, but it is a hexatriene. It is able to form β-, δ- and ζ-adducts, so it was interesting to check whether and what kind of adducts would be formed by reacting **1** with potassium cyanide and sodium methoxide. On the other hand, potassium cyanide and sodium methoxide adducts are typical carbanions, and we could apply the recently established scale factors [38] in order to obtain better results in the prediction of their IR spectra.

2. Experimental

The title compound **1** was prepared by the classical Lemke's method [1]. The cyanide and methoxide adducts **8–10** were prepared by dissolving **1** in DMSO and adding the solution to excess of dry KCN, and $NaOCH_3$ respectively, under argon. After 1 min intense stirring, the reaction mixtures were filtered by using a syringe-filter to remove the solid KCN or $NaOCH_3$. The clear adduct solutions were put immediately into CaF_2 cell of 0.129 mm path length. All experiments were repeated with DMSO-d_6 in order to provide measurements in the IR regions overlapped by the absorption of DMSO. The IR spectra were recorded on Bruker IFS 113v and Tensor 27 FT spectrometers at resolution of 1 cm^{-1} and 64 scans. The IR spectra were measured by intervals of 3 min within the first hour and by intervals of 10 min for the following 2 h.

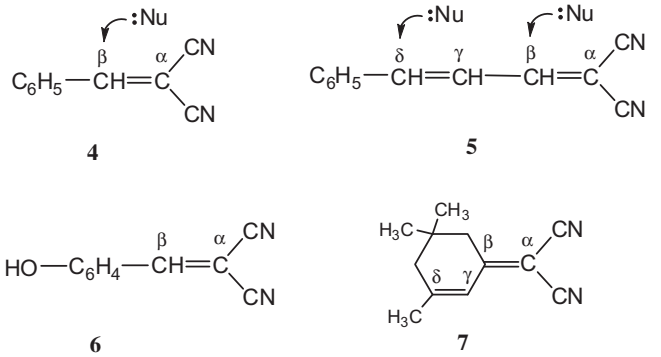

Scheme 2. Carbanionic adducts of benzylidenemalononitrile 4 and other strongly polarized alkenes **5–7.**

3. Computations

The Gaussian 98 program package [39] was used for Density Functional Theory (DFT, full optimization) computations of energies, structures and IR spectra of the species studied. This theory is the groundwork of a series of cost-effective methods to approximate electron correlation effects [40]. We employed the B3LYP functional, which combines Becke's three-parameter non-local exchange with the correlation functional of Lee et al. [40,41], adopting a 6-31++G** basis set with some symmetry restrictions. For each structure, the stationary points found on the molecular potential energy hypersurfaces were characterized using the standard analytical harmonic procedure. The absence of irrational frequencies or negative eigenvalues of the second-derivative matrix confirmed that the stationary points corresponded to global minima on the potential energy surfaces [40]. A standard least-square program was used for calculating the single-parameter linear regression indices.

4. Results and discussion

4.1. Energy analysis

We computed at B3LYP/6-31++G** theory level all possible structures of molecule **1**, and its cyanide **8a–10a** and methoxide adducts **8b–10b** (Scheme 3).

For the molecule **1** and its cyanide adducts we found only one stable conformer. The cyclohexene ring adopts very stable "envelope shaped" conformation (see formula **1** in the Introduction), which is not significantly altered after the addition of the corresponding nucleophile. This conformation is caused by the hindering effect of the both geminal methyl groups bonded at atom number 3 in the ring. Most of the atoms of **1** lie in a plane, except for the isopropyl fragment which is situated out of the respective plane. The methoxide adducts have several comformers, witch are due to the rotation of the newly added methoxy group. We selected only the most stable of them in this analysis. The C atoms in the molecule of **1** are diastereotopic (Scheme 3), so the addition of nucleophiles creates a chiral center and a couple of diastereoisomers for each one of them. The zero point corrected energies of these species are compared in Table 1. It can be seen that the energy differences between diastereoisomers are 0.44–7.29 kJ mol^{-1}, so they would exist together in the solution. According to the computations, R-diastereoisomers are more stable, than S-ones in most cases.

The computed energy differences between β–ζ, and δ–ζ adducts are 29–58 and 24–39 kJ mol^{-1} (Table 1). These differences are due to better resonance stabilization of the carbanionic charge in case of δ- and ζ-adducts. It is the main driving force causing the isomerisation, connected to generation of thermodynamic more stable products.

4.2. Correlation analysis

Comparison of the native B3LYP/6-31++G** vibrational frequencies of **1** with those we have measured in DMSO solvent (see spectral analysis below) resulted in the formation of an excellent ($0.99 < R < 1$) correlation (Eq. (1)):

$$\nu = 0.9286\omega + 66.1(cm^{-1}) \quad (1)$$

Correlation coefficient $R = 0.99996$
Standard deviation S.D = 6.37 cm^{-1}
Number of data points $n = 53$

We shall use Eq. (1) for correlational scaling [42] of the theoretical frequencies. As stated in Alcolea's review article [42] (and

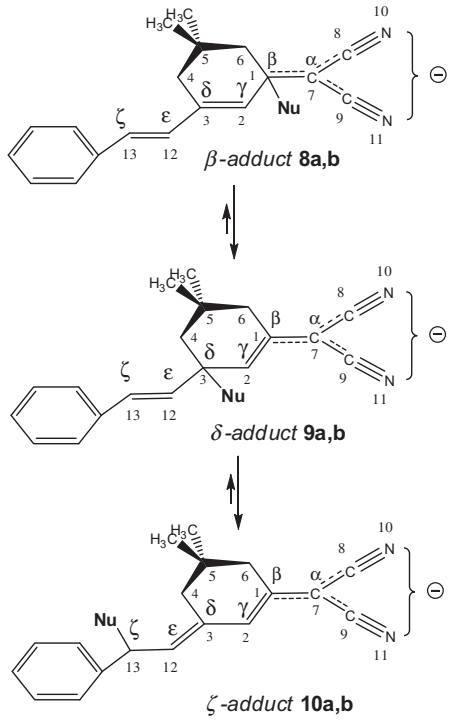

Scheme 3. β-, δ-, and ζ-Adducts of **1.**

Table 1
ZPVEnergies ($E^{ZPVEcorr.}$ in Hartree) and energy differences (ΔE in kJ mol^{-1}) of diastereoisomeric couples adducts of **1.**

Isomers	$E^{ZPVEcorr}$		ΔE^a
	R	S	
Cyanide adducts			
β-Adduct **8a**	−936.957409	−936.954631	−7.29
δ-Adduct **9a**	−936.963083	−936.962032	−2.76
ζ-Adduct **10a**	−936.977137	−936.976968	−0.44
ΔE^b	−51.80	−58.65	–
ΔE^c	−36.90	−39.21	–
Methoxide adducts			
β-Adduct **8b**	−959.208777	−959.207858	−2.41
δ-Adduct **9b**	−959.210815	−959.210298	−1.35
ζ-Adduct **10b**	−959.22011	−959.221971	4.87
ΔE^b	−29.75	−37.05	–
ΔE^c	−24.40	−30.65	–

[a] Energy difference between each particular diastereoisomeric couples.
[b] Energy difference between β- and ζ-isomers.
[c] Energy difference between δ- and ζ-isomers.

references therein), the use of scaling equations instead of overall scaling factors [43,44] gives better results, especially in the low-frequency region. For more recent works see [45–51] (and references therein).

4.3. Spectral analysis

4.3.1. Neutral compound *1*

Our theoretical and experimental (DMSO/DMSO-d_6) IR data for **1** are compared in Table 2 together with the approximate description of the corresponding vibrations. The C—H stretching vibrations appeared in their usual ranges (Table 2). As it could be expected the phenyl ν(C—H) vibrations were the most high-frequency ones among them. The strongest band in the spectrum of **1** at 1562 cm^{-1} corresponds to the $\nu(C^2{=}C^3)$ of the endocyclic double C=C bond (Table 2, vibration 24), mixed with phenyl ν(C=C). Another strong band due to $\nu(C^1{=}C^7)$ of the exocyclic double C=C bond is observed at 1525 cm^{-1}. These values are close to those, measured in solid state [8]. We found in the experimental spectrum a single moderate band in the ν(C≡N) region, without shoulders or satellites, at 2219 cm^{-1}. We have no doubts about existing of two bands, as a superposition of the ν^s(C≡N) and ν^{as}(C≡N), with frequencies very close to each other. After decomposition of the complex band, (see Fig. 1) we obtained two frequencies, differing by 5 cm^{-1}. The calculations predict larger splitting $\Delta\nu(C{\equiv}N)_2{=}\nu^s(C{\equiv}N)_2 - \nu^{as}(C{\equiv}N)_2$ of 13 cm^{-1} (Table 2, vibrations 19 and 20). The experimental value of this splitting is very similar to those found for dozens of ylidenemalonitriles [24–26] (and references therein). It is also known that in some cases the theory overestimates this splitting as for example with compound **7** [37] (see Section 1). However in general, the theoretical frequencies correspond very well to the experimental ones, whenever they were scaled with Eq. (1); the mean absolute deviation: $1/n\Sigma_{i=1}^{n}|\omega_i - \nu_i|$ (MAD in Table 2) is only 5.3 cm^{-1}. This value is low and gets out of the interval of 9–24 cm^{-1}, typical for MADs of IR frequencies computed by DFT functionals [48–51] (and references therein). By scaling with overall scale factors we obtained several times larger deviation.

We measured the IR intensities of the strongest bands in the spectrum of **1** (Nos. 19–22, 24, 25 in Table 2). The agreement with their theoretical values is only qualitative. This result corresponds to the observed by many authors [25–28,36,52,53]. In a recent study [38] we demonstrated, that quantitative theoretical prediction of IR intensities is possible by scaling, whenever we select relative spectral modes, measured in identical conditions. So, we applied the scaling equations established in [38], and the integrated intensities for ν^s(C≡N) and ν^{as}(C≡N), which we obtained in this way, show very good agreement between theory and experiment (see Nos. 19, 20 in Table 2). Unfortunately we did not find scaling factors or equation in literature, which could be used to scale the other theoretical intensities. Their native values are listed in Table 2.

4.3.2. Carbanionic adducts of *1*

Compound **1** reacts rapidly (within 1 min) with KCN and $NaOCH_3$. The bands of the starting **1** disappear and new bands appear in the IR spectra due to the formation of adducts **8–10**. The most informative part in whole IR spectrum is the region of cyano stretching vibrations (2300–2000 cm^{-1}). The bands, which we observed in this region, are typical for carbanions, containing dicyanomethanide fragments. The new stronger bands are blue shifted *c.a.* 50–100 cm^{-1} in comparison to the bands of molecule **1** and their frequencies are close to those, observed for adducts of compounds **4–7**. In the course of time, the CN stretching bands change their positions and intensities due to the conversion β → δ → ζ-adducts (Scheme 3). The isomerisation of β- to δ-adducts is monitored by small, but well visible increase in cyano stretching frequencies (5–15 cm^{-1} see Table 3 and Fig. 2). According to the calculations (Table 3, Fig. 2) the ν^s(C≡N) and ν^{as}(C≡N) bands of ζ-adducts **10a** and **10b** are additionally shifted to higher frequencies than δ-ones. They were also observed in the experimental spectra.

Whenever the nucleophile is potassium cyanide, (Scheme 3) the bands observed in the IR spectra correspond to β- and ζ-adducts (**8a** and **10a** in Table 3). Amounts of ζ-cyanide adduct were noticed only 3 min after the stirring had started. The β → ζ isomerisation goes off slowly, and does not finish completely within 3 h. Well shaped, strong bands indicating the presence of δ-cyanide adduct **9a** were not registered in this period. For that reason, we suppose that δ → ζ isomerisation is rather quick. We could not find as well

Table 2
Theoretical (B3LYP 6-31++G**) and experimental (solvent DMSO/DMSO-d_6) frequencies (ω, ν in cm^{-1}) and integrated intensities (A in km mol^{-1}) of DPCM molecule **1**.

No.	B3LYP/6-31++G**				Experimental data[a]	
	ω[b]	ω[c]	A	Approximate description[d]	ν	A[e]
1	3099	3055	22	ν_{C-H}(Ph)	3057	vw
2	3092	3048	21	ν_{C-H}(Ph)	3040	vw
3	3083	3040	10	ν_{C-H}(Ph)	[f]	–
4	3075	3032	6	ν_{C-H}(Ph)	3028	vw
5	3074	3031	1	ν_{C-H}(Ph)	[f]	–
6	3066	3023	17	$\nu^{cycohexen}_{=C-H}$	[f]	–
7	3061	3018	9	$\nu^{as\ vinyl}_{=C-H}$	[f]	–
8	3053	3011	3	$\nu^{as=\ vinyl}_{C-H}$	3010	m
9	3008	2967	27	$\nu^{as}(CH_3)$	2960	m
10	2998	2957	35	$\nu^{as}(CH_3)$	2935	m
11	2994	2953	11	$\nu^{as}(CH_3)$	[f]	–
12	2991	2950	23	$\nu^{as}(CH_3)$	[f]	–
13	2988	2948	4	$\nu^{as}(CH_3)$	[f]	–
14	2966	2926	14	$\nu^{as}(CH_2)$	[f]	–
15	2933	2894	19	$\nu^{s}CH_3$)	2895	w
16	2923	2885	34	$\nu^{s}CH_3$)	2872	w
17	2906	2868	12	$\nu^{as}(CH_2)$	[f]	–
18	2904	2867	12	$\nu^{as}(CH_2)$	[f]	–
19	2221	2227	55.4[g]	ν^{s}_{C-N}	2221	55.6
20	2207	2213	19.6[g]	ν^{as}_{C-N}	2216	23.8
21	1611	1614	45	$\nu^{vinyl}_{C=C}$	1614	14.7
22	1588	1592	7	$\nu_{C=C}$(Ph)	1598	7.1
23	1562	1568	2	$\nu_{C=C}$(Ph)	1562	230.4
24	1549	1555	519	$\nu^{endo}_{C=C}$		
25	1499	1507	328	ν^{exo}_{C-C}	1525	151.4
26	1477	1485	4	δ_{C-H}(Ph)	1496	w
27	1464	1473	6	$\delta^{s}(CH_3)$	1470	w
28	1458	1467	6	$\delta^{s}(CH_3)$	1470	w
29	1448	1457	5	$\delta^{as}(CH_3)$	[f]	–
30	1440	1449	2	$\delta^{as}(CH_3)$	[f]	–
31	1432	1442	13	δ_{C-H}(Ph)	1450	w
32	1425	1435	0	$\delta^{sciss.}(CH_2)$	[f]	–
33	1416	1426	6	$\delta^{sciss.}(CH_2)$	[f]	–
34	1382	1393	8	$\gamma(CH_3)$	1400	w
35	1376	1388	47	$\delta^{endo}_{=C-H}$	1390	w
36	1361	1373	10	$\gamma(CH_3)$	1370	w
37	1330	1343	4	$\gamma(CH_2)$	[f]	–
38	1326	1339	10	$\delta^{vinyl}_{=C-H}$; $\delta^{endo}_{=C-H}$	[f]	–
39	1319	1332	8	δ_{C-C}(Ph); δ_{C-H}(Ph)	[f]	–
40	1315	1328	102	δ_{C-H}(Ph); ν_{C-C}(Ph)	1334	m
41	1298	1312	56	$\gamma(CH_2)$; $\delta^{vinyl}_{=C-H}$	1313	w
42	1278	1292	2	$\gamma(CH_2)$; $\delta^{endo}_{=C-H}$	[f]	–
43	1274	1288	20	$\gamma(CH_2)$; ν_{C-C}	1296	w
44	1257	1272	2	δ_{C-H}; ν_{C-C}	[f]	–
45	1241	1257	1	ν_{C-C}; δ_{C-H}	[f]	–
46	1214	1231	9	$\delta^{endo}_{=C-H}$; δ_{C-H}	[f]	–
47	1182	1199	52	$\delta_{=C-H}$(Ph)	1201	w
48	1166	1184	13	$\delta_{=C-H}$(Ph)	1184	w
49	1161	1179	38	ν_{C-CN}; δ_{C-H}	1184	w
50	1146	1165	8	$\gamma^{twist.}(CH_2)$; ν_{C-C}	1161	w
51	1145	1164	3	$\delta_{=C-H}$(Ph)	1161	w
52	1141	1160	36	$\gamma^{twist.}(CH_2)$; ν_{C-C}	1161	w
53[h]	1113	1133	4	ν_{C-C}; $\gamma^{twist.}(CH_2)$	1133	w
MAD	***24.12***	***5.33***	–	–	–	–

[a] Measured after having decomposed the complex bands into components.
[b] Scaled by 0.9552 for $\nu_{C\equiv N}$ [38] and by 0.9648 [43] for each other frequencies.
[c] Scaled, according to correlation Eq. (1).
[d] Vibrational modes: ν, stretching; δ, in-plane bending; γ, out-of-plane bending; superscripts: s, symmetrical; as, asymmetrical; sciss, scissoring; wag, wagging; endo, endocyclic; exo, exocyclic.
[e] Relative intensities: m, moderate; w, weak; v, very.
[f] These bands were not detected in the experimental spectrum.
[g] Scaled by 0.2825A + 8.3 [38].
[h] Followed by 58 lower-frequency vibrations.

ν(C≡N) bands due to the newly added cyano group, although similar bands were detected in some cases [25,27,37]. This group is non-polar and conjugated with the carbanionic centers and the other multiple bonds, so its intensity is expected to be low. According to the computations these bands would be 10–20 times weaker than the others.

Whenever the nucleophile is sodium metoxide, (Scheme 3) 3 min after the stirring starts, the bands observed in the IR spectra

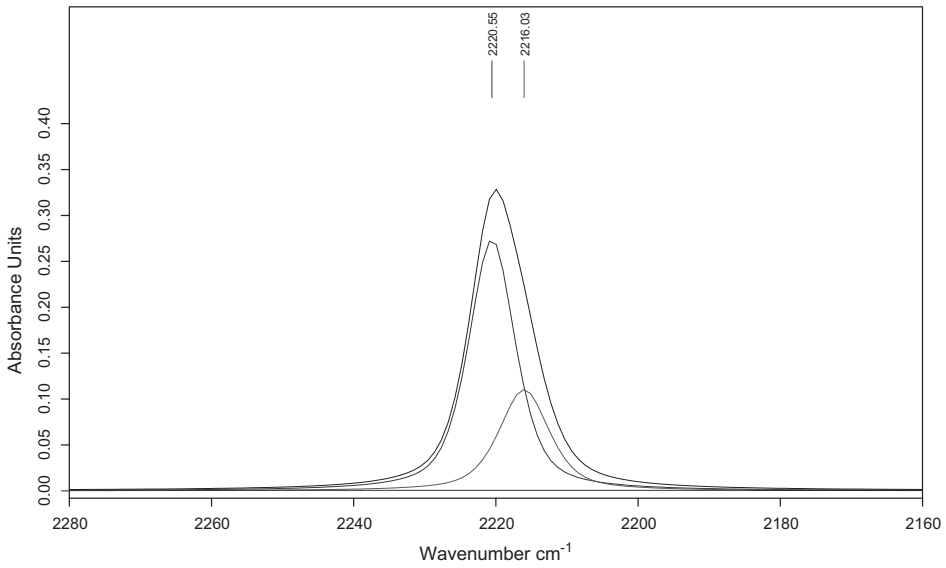

Fig. 1. Measurement of cyano stretching frequencies after decomposition of the complex band into components ($\nu^{s}_{C\equiv N} = 2221\ cm^{-1}$, and $\nu^{as}_{C\equiv N} = 2216\ cm^{-1}$).

Table 3
Theoretical (B3LYP 6-31++G**) and experimental (solvent DMSO) cyano stretching IR frequencies (ω, ν in cm^{-1}) and integrated intensities (A in km mol^{-1}) of cyanide and methoxide carbanionic adducts of DPCM **8–10**.

No.	B3LYP 6-31++G **				Experimental data[a]	
	ω[b]	ω[c]	A[d]	Approximate description[e]	ν	A[f]
8a *β-Cyanide adduct*						
1	2165	2151	100.0	$\nu^{s}_{C\equiv N}$	2157	vs
2	2111	2105	230.4	$\nu^{as}_{C\equiv N}$	2100	vs
9a *δ-Cyanide adduct*						
1	2180	2165	167.5	$\nu^{s}_{C\equiv N}$	–[g]	–[g]
2	2142	2129	190.6	$\nu^{as}_{C\equiv N}$	–[g]	–[g]
10a *ζ-Cyanide adduct*						
	2186	2171	210.1	$\nu^{s}_{C\equiv N}$	2164	vs
	2150	2138	172.0	$\nu^{as}_{C\equiv N}$	2122	vs
8b *β-Methoxide adduct*						
1	2164	2150	128.8	$\nu^{s}_{C\equiv N}$	–[g]	–[g]
2	2120	2108	223.9	$\nu^{as}_{C\equiv N}$	–[g]	–[g]
9b *δ-Methoxide adduct*						
1	2179	2165	201.2	$\nu^{s}_{C\equiv N}$	2160	vs
2	2140	2128	193.4	$\nu^{as}_{C\equiv N}$	2112	vs
10b *ζ-Methoxide adduct*						
1	2184	2169	206.1	$\nu^{s}_{(C\equiv N)_2}$	2164	vs
2	2148	2135	173.8	$\nu^{as}_{(C\equiv N)_2}$	2123	vs
MAD	**19.3**	**9.1**				

[a] Measured after having decomposed the complex bands into components.
[b] Scaled by 0.9642 [38].
[c] Scaled, according to correlation Eq. (1).
[d] Scaled by 0.2825A + 8.3 [38].
[e] Vibrational modes: ν, stretching; superscripts: s, symmetrical; as, asymmetrical.
[f] Relative intensities: w, weak; vs very strong.
[g] We did not find measurable amounts of this adduct.

show complete isomerisation to δ-adduct **9b**, and even partial isomerisation to ζ-adduct **10b**. This result is very similar to that, observed for the methoxide adducts of compound **7** [37]. The δ → ζ isomerisation goes off slowly, and does not finish completely within 3 h. After this period, new undesired bands appear in the region of 2300–2000 cm^{-1}, indicating some further chemical conversions of the adducts. ν^{as}(CH) and ν^{s}(CH) of the newly added methoxy group are noticed like broad moderate bands at *c.a.* 2950 and 2900 cm^{-1} respectively, and cannot be separated completely from the other CH vibrations. The conversion of molecule **1** into ζ-methoxide adduct **10b** caused the appearance of two strong bands at 1599 and 1538 cm^{-1}, corresponding to $\nu(C^3{=}C^{12})$ and $\nu(C^1{=}C^2)$ vibrations.

The experimental and theoretical data about nitrile stretching vibration of the studied species are compared in Table 3. Scaling of the nitrile frequencies with specific scale factors for them [38], gives better results than scaling with overall scale factors [44]. The mean absolute deviation in the former case is 19.3 cm^{-1}, which is however larger than the average observed in series of 44 anions, containing cyano groups [38]. In order to improve the agreement, we used correlation Eq. (1) and obtained much better accuracy. Due to the simultaneous presence of the various adducts

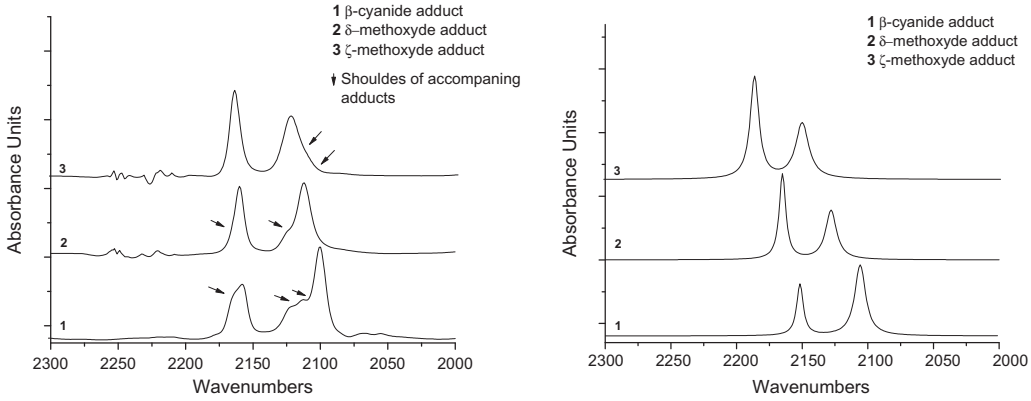

Fig. 2. Experimental (left) and theoretical (right) IR spectra of various adducts of **1** in nitrile stretch region 2300–2000 cm^{-1}.

Table 4
Selected bond lengths R (Å) and bond angles A (degrees) of **1** and of its cyanide and methoxide adducts.

Bonds and angles[a]	Molecule	Cyanide adducts	Methoxide adducts	Δ[b]	∇[c]
β-Adducts					
	1	**8a**	**8b**		
R (3,2)	1.371	1.353	1.355	−0.018	−0.016
R (3,12)	1.449	1.458	1.455	0.009	0.006
R (2,1)	1.434	1.519	1.506	0.085	0.072
R (1,7)	1.384	1.544	1.518	**0.160**	**0.134**
R (7,8)	1.429	1.400	1.403	−0.029	−0.026
R (8,10)	1.166	1.178	1.178	0.012	0.012
R (12,13)	1.357	1.355	1.357	−0.002	0.000
A (1,2,3)	123.1	125.5	125.8	2.4	2.7
A (1,7,8)	121.9	120.8	121.7	−1.1	−0.2
A (2,1,7)	121.3	108.1	108.3	**−13.2**	**−13**
A (2,3,12)	118.6	118.4	118.7	−0.2	0.1
A (3,12,13)	127.1	126.8	126.8	−0.3	−0.3
δ-Adducts					
	1	**9a**	**9b**		
R (3,2)	1.371	1.523	1.506	**0.152**	**0.135**
R (3,12)	1.449	1.526	1.516	0.077	0.067
R (2,1)	1.434	1.365	1.366	−0.069	−0.068
R (1,7)	1.384	1.449	1.450	0.065	0.066
R (7,8)	1.429	1.411	1.411	−0.018	−0.018
R (8,10)	1.166	1.175	1.176	0.009	0.010
R (12,13)	1.357	1.344	1.344	−0.013	−0.013
A (1,2,3)	123.1	125.0	125.5	1.9	2.4
A (1,7,8)	121.9	121.8	122.0	−0.1	0.1
A (2,1,7)	121.3	123.3	123.5	2.0	2.2
A (2,3,12)	118.6	108.4	108.3	**−10.2**	**−10.3**
A(3,12,13)	127.1	126.2	126.3	−0.9	−0.8
ζ-Adducts					
	1	**10a**	**10b**		
R (3,2)	1.371	1.440	1.438	0.069	0.067
R (3,12)	1.449	1.367	1.371	−0.082	−0.078
R (2,1)	1.434	1.378	1.378	−0.056	−0.056
R (1,7)	1.384	1.438	1.439	0.054	0.055
R (7,8)	1.429	1.413	1.413	−0.016	−0.016
R (8,10)	1.166	1.174	1.175	0.008	0.009
R (12,13)	1.357	1.516	1.497	**0.159**	**0.140**
A (1,2,3)	123.1	124.4	124.4	1.3	1.3
A (1,7,8)	121.9	121.9	122.0	0.0	0.1
A (2,1,7)	121.3	123.5	123.5	2.2	2.2
A (2,3,12)	118.6	120.9	121.4	2.3	2.8
A (3,12,13)	127.1	113.5	114.4	**−13.6**	**−12.7**

[a] Atom numbering according to formula **1** in Introduction.
[b] Δ = value (cyanide adduct) − value (molecule).
[c] ∇ = value (methoxide adduct) − value (molecule). The largest $|\Delta|$ and $|\nabla|$ values are given in bold.

in the solution and their overlapping nitrile stretch bands, it was impossible to measure the integral intensities of the ν(C≡N) bands for each adduct. Their scaled theoretical values (Table 3) are similar to the experimental ones, observed for adducts of **7**. They show a relative increase of the intensity of ν^{s}(C≡N) compared to ν^{as}(C≡N) by the conversion of β- into δ- and ζ-adducts which was confirmed by the experimentally observed intensities of the nitrile stretch bands as illustrated in Fig. 2. For these reasons, we may consider the IR intensities of these bands as reliably predicted by the theory.

Table 5
Net NBO charges on selected atoms in **1** and its adducts.

Atoms[a]	Molecule	Cyanide adducts	Methoxide adducts	Δ[b]	∇[c]
β-Adducts					
1	0.09	−0.18	−0.23	**−0.27**	**−0.32**
2	−0.24	−0.12	−0.12	0.12	0.12
3	0.03	−0.08	−0.10	−0.11	−0.13
7	−0.29	−0.48	−0.50	**−0.19**	**−0.21**
8	0.28	0.28	0.29	0.00	0.01
9	0.28	0.29	0.30	0.01	0.02
10	−0.30	−0.47	−0.48	**−0.17**	**−0.18**
11	−0.30	−0.47	−0.47	**−0.17**	**−0.17**
12	−0.22	−0.16	−0.15	0.06	0.07
13	−0.15	−0.24	−0.26	−0.09	−0.11
14	−0.10	−0.07	−0.07	0.03	0.03
δ-Adducts					
1	0.09	0.03	0.03	−0.06	−0.06
2	−0.24	−0.33	−0.37	−0.09	−0.13
3	0.03	−0.22	0.21	**−0.25**	**0.18**
7	−0.29	−0.46	−0.47	**−0.17**	**−0.18**
8	0.28	0.29	0.29	0.01	0.01
9	0.28	0.31	0.31	0.03	0.03
10	−0.30	−0.46	−0.47	**−0.16**	**−0.17**
11	−0.30	−0.45	−0.45	**−0.15**	**−0.15**
12	−0.22	−0.15	−0.16	0.07	0.06
13	−0.15	−0.26	−0.26	−0.11	−0.11
14	−0.10	−0.06	−0.05	0.04	0.05
ζ-Adducts					
1	0.09	0.04	0.04	−0.05	−0.05
2	−0.24	−0.33	−0.33	−0.09	−0.09
3	0.03	−0.01	0.00	−0.04	−0.03
7	−0.29	−0.44	−0.44	**−0.15**	**−0.15**
8	0.28	0.29	0.30	0.01	0.02
9	0.28	0.31	0.31	0.03	0.03
10	−0.30	−0.45	−0.45	**−0.15**	**−0.15**
11	−0.30	−0.44	−0.44	**−0.14**	**−0.14**
12	−0.22	−0.31	−0.33	−0.09	−0.11
13	−0.15	−0.38	0.03	**−0.23**	**0.18**
14	−0.10	−0.02	−0.04	0.08	0.06

[a] Atom numbering according to formula **1** in Introduction.
[b] Δ = value (cyanide adduct) − value (molecule).
[c] ∇ = value (methoxide adduct) − value (molecule). The largest $|\Delta|$ and $|\nabla|$ values are given in bold.

4.4. Structural analysis

The conversion of **1** into adducts is not accompanied by essential changes in the general form of the parent molecule. However the structural elements in the fragment, where the reactions take place, undergo essential variations (Table 4). Large bond length changes take place in cases when double or quasi-double bonds become single ones and vice versa, e.g. R (2,3) R (1,7) and R (12,13). The largest bond angle variations take place at atoms, which change their configurations from trigonal (sp^2) into tetrahedral (sp^3), e.g. A (2,1,7) A (2,3,12) and A (3,12,13).

The net atomic charges (Table 5) are in agreement with the bond length and bond angle variations (cf. Table 4). The largest charge changes take place at those atoms, which alter their configuration in the reaction course (atoms C^1, C^3, C^2, C^{12} and C^{13}). The conversion of the molecule **1** into adducts leads to an increase of the electronic density upon N atoms with 0.14–0.17 e^-.

5. Conclusion

The combined IR experimental/B3LYP computational approach, applied in the present work, allowed to prove both the conversion of 2-{5,5-dimethyl-3-[(2-phenyl)vinyl]cyclohex-2-enylidene}-malononitrile into potassium cyanide and sodium methoxide adducts, as well as the chemical driving force which is the main groundwork of the β-adduct → δ-adduct and δ-adduct → ζ-adduct isomerisations: the much higher stability (i.e. lower total energy) of the δ-adducts, compared to the β-ones, and of the ζ-adducts, compared to the δ-ones.

References

[1] R. Lemke, Chem. Ber. 103 (1970) 1168.
[2] R. Lemke, Chem. Ber. 103 (1970) 1894.
[3] R. Lemke, Synthesis (1974) 359.
[4] R. Wortmann, P.M. Lundquist, R.J. Twieg, C. Geletneki, C.R. Moylan, Y. Jia, R.G. DeVoe, D.M. Burland, M.P. Bernal, H. Coufal, R.K. Grigier, J.A. Hoffnagle, C.M. Jefferson, R.M. Macfarlane, R.M. Shelby, G.T. Sincerbox, Appl. Phys. Lett. 69 (1996) 1657.
[5] O.-P. Kwon, B. Ruiz, A. Choubey, L. Mutter, A. Schneider, M. Jazbinsek, V. Gramlich, P. Günter, Chem. Mater. 18 (2006) 4049.
[6] S.-J. Kwon, M. Jazbinsek, O.-P. Kwon, P. Günter, Cryst. Growth Des. 10 (2010) 1552.
[7] E. Kleinpeter, A. Koch, B. Mikhova, B. Stamboliyska, T. Kolev, Tetrahedron Lett. 49 (2008) 1323.
[8] T.M. Kolev, D.Y. Yancheva, B.A. Stamboliyska, Spectrochim. Acta A 59 (2003) 3325.
[9] B.M. Graven, C. Cusatin, G.L. Gartland, E.A. Vizzini, J.Mol. Struct. 16 (1973) 331.
[10] A.J. Barnes, L. Le Gall, J. Lauransan, J. Mol. Struct. 56 (1979) 29.
[11] Yu.N. Sheinker, Yu.I. Pomerantsev, Zh. Fiz. Khim. 23 (1959) 1819.
[12] T. Kolev, Z. Glavcheva, D. Yancheva, Acta Crystallogr. E57 (2001) 760.
[13] T. Kolev, Z. Glavcheva, M. Schuerman, Acta Crystallogr. E57 (2001) 964.
[14] T. Kolev, Z. Glavcheva, D. Yancheva, Acta Crystallogr. E57 (2001) 966.
[15] T. Kolev, Z. Glavcheva, M. Schuerman, Acta Crystallogr. E57 (2001) 1166.
[16] T. Kolev, D. Yancheva, M. Schuerman, Acta Crystallogr. E58 (2002) 1093.
[17] T. Kolev, D. Yancheva, B. Shivachev, R. Petrova, M. Spiteler, Acta Crystallogr. E58 (2002) 1093.
[18] S. Patai, Z. Rappoport, in: S. Patai (Ed.), The chemistry of the alkenes, Interscience, London, 1964 (Chapter 8).
[19] D.J. Kroeger, R. Stewart, Can. J. Chem. 45 (1967) 2163.
[20] R. Stewart, D.J. Kroeger, Can. J. Chem. 45 (1967) 2173.
[21] C.A. Fyfe, Can. J. Chem. 47 (1969) 2331.
[22] I.N. Juuchnovski, I.G. Binev, Tetrahedron Lett. (1974) 3645.
[23] I.G. Binev, I.N. Juchnovski, Bulg. Chem. Commun. (Izv. Khim.) 9 (1976) 33.
[24] I.N. Juchnovski, I.G. Binev, Bull. Soc. Chim. Belg. 86 (1977) 793.
[25] I.N. Juchnovski, V.B. Radomirska, I.G. Binev, Bulg. Chem. Commun. (Izv. Khim.) 14 (1981) 147.
[26] I.G. Binev, Y.I. Binev, B.A. Stamboliyska, I.N. Juchnovski, J. Mol. Struct. 435 (1997) 235.
[27] E.A. Velcheva, I.E. Bineva, I.N. Juchnovski, C. R. Acad. Bulg. Sci. 51 (5-6) (1998) 41.
[28] E.A. Velcheva, Y.I. Binev, M.J. Petrova, J. Mol. Struct. 475 (1999) 65.
[29] E.A. Velcheva, Bulg. Chem. Commun. 32 (2000) 162.
[30] Z.I. Demireva, I.G. Binev, I.N. Juchnovski, Tetrahedron Lett. (1972) 1713.
[31] Z. Rappoport, S. Gerter, J. Chem. Soc. (1964) 1360.
[32] D.A. Scola, J.S. Adams Jr., J. Chem. Eng. Data 15 (1970) 349.
[33] B.A. Arbuzov, N.A. Poleznaev, V.S. Vinogradova, I.I. Saydashev, Izv. Akad. Nauk SSSR, Ser. Khim. (1971) 2762.
[34] C.A. Fyfe, M. Zbozny, Can. J. Chem. 50 (1972) 1713.
[35] G. Ferguson, C.A. Fyfe, W.C. March, Can. J. Chem. 51 (1973) 2794.
[36] Y.I. Binev, I.G. Binev, I.N. Juchnovski, J. Mol. Struct. (THEOCHEM) 532 (2000) 31.
[37] S.S. Stoyanov, A.D. Popova, J.A. Tsenov, Bulg. Chem. Commun. 40 (2008) 538.
[38] S.S. Stoyanov, J. Phys. Chem. A 114 (2010) 5149.
[39] M.J. Frisch, G.W. Trucks, H.B. Schlegel, G.E. Scuseria, M.A. Robb, J.R. Cheeseman, V.G. Zakrzewski, J.A. Montgomery Jr., R.E. Stratmann, J.C. Burant, S. Dapprich, J.M. Millam, A.D. Daniels, K.N. Kudin, M.C. Strain, O. Farkas, J. Tomasi, V. Barone, M. Cossi, R. Cammi, B. Mennucci, C. Pomelli, C. Adamo, S. Clifford, J. Ochterski, G.A. Petersson, P.Y. Ayala, Q. Cui, K. Morokuma, K. D. Malick, A.D. Rabuck, K. Raghavachari, J.B. Foresman, J. Cioslowski, J.V. Ortiz, A.G. Baboul, B.B. Stefanov, G. Liu, A. Liashenko, P. Piskorz, I. Komaromi, R. Gomperts, R.L. Martin, D.J. Fox, T. Keith, M.A. Al-Laham, C.Y. Peng, A. Nanayakkara, C. Gonzalez, M. Challacombe, P.M.W. Gill, B. Johnson, W. Chen, M.W. Wong, J.L. Andres, M. Head-Gordon, E.S. Replogle, J.A. Pople, Gaussian 98, Revision A.7, Gaussian, Inc., Pittsburgh PA, 1998.
[40] A.D. Becke, J. Chem. Phys. 98 (1993) 5648.
[41] C. Lee, W. Yang, G.R. Parr, Phys. Rev. Part B 37 (1988) 785.
[42] A. Alcolea Palafox, Rec. Res. Develop. Phys. 2 (1998) 213.
[43] A. Scott, L. Radom, J. Phys. Chem. A 100 (1996) 16502.
[44] J. Merrick, D. Moran, L. Radom, J. Phys. Chem. A 111 (2007) 11683.
[45] I.D. Reva, S.V. Ilieva, R. Fausto, Phys. Chem. Chem. Phys. 3 (2001) 4235.
[46] O. Sala, N.S. Gonsalves, L.K. Nada, J. Mol. Struct. 565–566 (2001) 411.
[47] M. Alcolea Palafox, V.K. Rastogi, L. Mittal, Int. J. Quant. Chem. 94 (2003) 198.
[48] M.K. Georgieva, P.A. Angelova, I.G. Binev, J. Mol. Struct. 692 (2003) 23.
[49] L.I. Daskalova, I.G. Binev, Int. J. Quant. Chem. 106 (2006) 1338.
[50] L.I. Daskalova, E.A. Velcheva, I.G. Binev, J. Mol. Struct. 826 (2007) 198.
[51] L.I. Daskalova, J. Mol. Struct. (THEOCHEM) 848 (2008) 9.
[52] B. Galabov, T. Dudev, Vibrational intensities, Elsevier Science, Amsterdam, 1996.
[53] M. Halls, H. Schlegel, J. Chem. Phys. 109 (1998) 10587.